Nanomed. J. 10(3): 197-209, Summer 2023

RESEARCH PAPER

Effect of polycaprolactone/carbon nanotube scaffold implantation along with liposomal ellagic acid in hippocampal synaptogenesis after spinal cord injury

Arman Abroumand Gholami [1, 2], Fatemeh Gheybi [3, 4], Amir Mahdi Molavi [5], Fatemeh Tahmasebi [1], Arash Papi [4], Hamideh Babaloo [6]*

[1]Department of Anatomy and Cell Biology, School of Medicine, Mashhad University of Medical Sciences, Mashhad, Iran
[2]Neuroscience Research Center, Mashhad University of Medical Sciences, Mashhad, Iran
[3]Department of Medical Biotechnology and Nanotechnology, Faculty of Medicine, Mashhad University of Medical Sciences, Mashhad, Iran
[4]Nanotechnology Research Center, Pharmaceutical Technology Institute, Mashhad University of Medical Sciences, Mashhad, Iran
[5]Department of Materials Research, Iranian Academic Center for Education, Culture and Research, Khorasan Razavi Branch, Mashhad, Iran
[6]Regenerative Medicine, Organ Procurement and transplantation Multi-Disciplinary Center, Razi Hospital, School of Medicine, Guilan University of Medical Sciences, Rasht, Iran

ABSTRACT

Objective(s): Memory and cognition impairments are the most important secondary effects of spinal cord injury (SCI) in the hippocampus. Therefore, the present study aimed to examine the effect of implantation of polycaprolactone/ functionalized multiwall carbon nanotube (PCL/f-MWCNT) scaffold along with ellagic acid loaded liposome (EA@lip) in neurological function recovery and hippocampus deficit after SCI.

Materials and Methods: Twenty-four female Wistar rats were randomly assigned into 4 groups (n=6): Ctrl- group (laminectomy without SCI), Ctrl+ group (SCI), PCL/CNT group (implantation of PCL/f-MWCNT scaffold) and PCL/CNT/EA group (implantation of PCL/f-MWCNT/EA@lip scaffold). The injury model was the dorsal hemisection at the T9 level. Characterization of EA@lip made by remote loading method was done by transmission electron microscopy and dynamic light scattering. Also, the morphology of PCL/f-MWCNT fibers was investigated by field-emission scanning electron microscopy (FE-SEM). Behavioral tests were used to evaluate the neurobehavioral performance of the animals. After 4-weeks, excitatory postsynaptic potential was recorded from the CA1 area of the hippocampus. Hippocampal mRNA levels of amyloid beta precursor protein (APP), cyclic nucleotide phosphodiesterase (CNP), glutamate ionotropic receptor kainate type subunit 2 (GRIK2) and syntaxin-binding protein 1 (Munc 18-1) were assayed using reverse transcription-quantitative polymerase chain reaction (RT-qPCR).

Results: We demonstrated that, after implanting the PCL/CNT scaffold with or without EA@lip, the hippocampal action potential improved by increasing the slope and amplitude of fEPSP compared to the Ctrl+ group. RT-qPCR data showed that the expression of CNP and Munc 18-1 increased, and the expression of APP and GRIK2 decreased, in the groups that received PCL/CNT with or without EA@lip compared to the injury group. We also proved that the treatment with PCL/CNT/EA@lip improved behavioral performance compared to the Ctrl+ and PCL/CNT groups.

Conclusion: This study demonstrated that PCL/f-MWCNT/EA@lip scaffold implantation improves functional potential and alters the expression of memory-related genes in the hippocampus post-injury.

Keywords: *Action potentials, Drug delivery systems, Memory, Neurogenesis, Tissue engineering*

How to cite this article
Abroumand Gholami A, Gheybi F, Molavi AM, Tahmasebi F, Papi A, Babaloo H. Effect of polycaprolactone/carbon nanotube scaffold implantation along with liposomal ellagic acid in hippocampal synaptogenesis after spinal cord injury. Nanomed J. 2023; 10(3): 197-209. DOI: 10.22038/NMJ.2023.72151.1776

* *Corresponding author: Email: hbabaloo92@gmail.com*
Note. This manuscript was submitted on April 3, 2023;
approved on June 10, 2023

INTRODUCTION

As a consequence of spinal cord injury (SCI), patients experience significant impairments in movement and sensation, which can lead to various physical and psychological challenges. Previous research has indicated that cognitive impairments are also common among people with SCI, even when they do not have brain injuries [1]. These impairments are often associated with the hippocampus, a brain structure that plays a crucial role in memory and learning and depends on high levels of neuroplasticity [2]. The hippocampus is affected by SCI in both rodents and humans [3], but the mechanisms underlying this effect are not well understood. Some possible factors include inflammation and reduced synaptic plasticity and action potentials in the hippocampus [4, 5]. Moreover, the effect of SCI on hippocampal neurogenesis is unclear, as different studies have reported different results. However, it seems that the changes in the expression of amyloid beta precursor protein (APP), cyclic nucleotide phosphodiesterase (CNP), glutamate ionotropic receptor kainate type subunit 2 (GRIK2), and syntaxin-binding protein 1 (Munc 18-1) genes, which are related to the neuronal activity of hippocampal neurons, can be a sign of secondary damage to the hippocampus [6–9]. The APP gene encodes the amyloid precursor protein, which is cleaved by enzymes to produce amyloid-β (Aβ) peptides. The hippocampus is selectively vulnerable to Aβ accumulation and neuroinflammation, which can impair synaptic plasticity and neuronal survival [6]. The GRIK2 gene is a member of the glutamate receptor family that is regulated by synaptic activity and is involved in synaptic plasticity and memory [8]. Some studies have shown that the change of GRIK2 gene expression in hippocampal disorders may be due to the accumulation of Aβ peptides, brain inflammation and neuronal damage in the hippocampus [10, 11]. The CNP gene is involved in the metabolism of cyclic nucleotides and the formation of the myelin sheath in the CNS. In addition, the expression of the CNP gene is altered in animal models of cognitive and memory disorders, especially in the hippocampus, indicating its possible role in synaptic plasticity and memory [7, 12, 13]. The Munc 18-1 gene encodes a protein that interacts with syntaxin 1 and regulates synaptic vesicle fusion in neurons. This gene is essential for the release of neurotransmitters and synaptic transmission in the hippocampus [9]. Neurogenesis is known to be important for memory and cognition in non-SCI models [14]. Hence, it is essential to consider strategies that aim to enhance and restore hippocampal function in the therapeutic approaches for SCI.

Synthetic biomaterial substrates have been introduced as a way to provide structural support and control the growth of cells in tissue. The environment's chemical and physical properties affect how neurons grow, so the best conditions for cell growth and functional development are those that are similar to the natural environment of the local tissue [15]. Electrospun fiber scaffolds are a promising method to create a similar environment for local cells for implantation in tissue reconstruction [16]. Polycaprolactone (PCL) is one of the most common polymer materials for neural substrates, because it has high biocompatibility, non-toxic biodegradation properties, high stiffness, and relatively low degradation rate [17]. Therefore, the PCL composite scaffold can support the structural integrity for a long time *in vivo* [18, 19].

One of the key challenges for designing nerve guidance conduits that can mimic the natural environment of nerve tissues is to achieve electroconductivity, which can modulate the neuronal activity and enhance the neural regeneration [20]. Carbon nanotubes (CNTs) are a promising nanomaterial for incorporating into polymeric scaffolds for neural tissue engineering, due to their cylindrical shape, high conductivity, and large surface area [21]. By adding CNTs into PCL the electroconductivity and neurite outgrowth of the scaffold can be significantly improved [18]. Although multi-walled CNTs (MWCNTs) have limited biological applications due to their hydrophobic nature, they do not have the problems associated with CNTs-induced toxicity [22]. In order to increase the hydrophilicity and to avoid fiber aggregation, it is essential to functionalized MWCNTs (f-MWCNT) with COOH [23].

Ellagic acid (EA) is a plant-derived polyphenol that has diverse pharmacological effects, such as anti-inflammatory, anti-oxidant and cardioprotective activities [24]. Recently, it has been shown that EA can also protect the nervous system from aging, dysfunction and degeneration. EA has been reported to improve cognitive function and prevent neurodegeneration of Alzheimer's disease [25] memory and behavior or mental health disorders are considered as the most

frequent effects of severe and moderate TBI. It has been reported that ellagic acid (EA. Furthermore, EA has been suggested to have neuroprotective effects against ischemic stroke [26]. However, its clinical use is limited by its low bioavailability and poor water solubility, which reduce its therapeutic efficacy. Liposomes can provide a solution to this problem by releasing the EA in a controlled manner, which would enhance its chemical stability, delivery accuracy, and tissue regeneration potential by improving its absorption [27].

Therefore, in the present research, we investigated the efficacy of PCL/f-MWCNT scaffold along with EA loaded liposome (EA@lip) after SCI on hippocampal through behavioral performance assessment and its correlation with hippocampal neurogenesis and functional potential in rats.

MATERIALS AND METHODS

Synthesis of EA loaded liposome

In this study, EA@lips were prepared using the lipid film hydration and extrusion method. The lipid details containing hydrogenated soy phosphatidylcholine (HSPC): cholesterol (Chol): distearoyl-Glycero-3-Phosphoethanolamine-methoxy polyethylene glycol2000 (DSPE-mPEG2000) (Alabaster, USA) at molar ratios of 55:40:5 were prepared in a chloroform solvent, and the organic solvent was removed by rotary evaporator. Subsequently, to completely remove the solvent, a thin layer of lipid film was freeze-dried. Hydration was then carried out using dextrose solution (5%, pH=7.4) to form multi-lamellar vesicles, that were then dispersed by vortex at 65 °C. After liposome dialysis in dextrose solution, ellagic acid in dextrose was added, and the solution was incubated for one hour at 60 °C. The unentrapped EA was separated using centrifugation (5 min, 1500 rpm) followed by dialysis. Filtration with a syringe filter (pore size=0.2 µm) was done to sterilize EA@lip [28].

Characterization of EA@lip

The size and morphology of the EA@lip were characterized with dynamic light scattering (DLS) (Microtrac, Japan) and transmission electron microscopy (TEM) (JPK, Germany).

Scaffold fabrication

PCL with average Mn = 80,000 (Sigma-Aldrich) and functionalized MWCNT (f-MWCNT) (US Research Nanomaterials, USA) were dissolved in chloroform-methanol solvents (Sigma-Aldrich). The ratio of chloroform: methanol and PCL: f-MWCNT were set to 3:1 (v/v) and 100:3 (w/w), respectively. Also, the final concentration of the electrospinning was adjusted to 14% (w/v). Electrospinning of the solution was carried out using Fanavaran Nano-Meghyas Co (Iran). The apparatus parameters including high-voltage, needle to collector distance, collector rotation speed, and solution flow rate were kept constant at 30 kV, 15 cm, 800 rpm, and 1 ml/h.

Characterization of scaffolds

Field emission scanning electron microscopy (FE-SEM) (Supra 35VP-24-58, Germany) was used to assess the morphology and structural nature of PCL/f-MWCNT scaffold with and without EA@lip. The average diameter of the fibers in FE-SEM images was determined by the image J software. Fiber diameters are presented as mean ± SD.

Animal study

In this study, twenty-four female Wistar rats with weights in the range of 220-300 g were utilized. These rats were kept separately in cages under 12-hr light/dark cycles, and with free access to food and water. All procedures related to animals were approved by the Animal Ethics Committee of Mashhad University of Medical Sciences (Mashhad, Iran) and were carried out in accordance with the National Institute of Health guidelines for the care and use of laboratory animals and the guidelines of the Iranian Institutional Animal Ethics Committee (IR.MUMS.REC.1399.571).

Surgical procedure

An injection of ketamine (100 mg/kg; i.p) and xylazine (5 mg/kg; i.p) was given to anesthetize the rats. Before surgery, 2 mg/kg meloxicam was injected subcutaneously as an analgesic. Dorsal hemi-section method was used to induce SCI as described by Babaloo et al. [29]overcoming the consequences of SCI including the recovery of sensory and motor functions is considered to be a difficult tasks that requires attention to multiple aspects of treatment. The breakthrough in tissue engineering through the integration of biomaterial scaffolds and stem cells has brought a new hope for the treatment of SCI. In the present study, human endometrial stem cells (hEnSCs. After midline incision, a T9 laminectomy was carried

out. Subsequently, the exposed dura was incised longitudinally and pulled laterally following a T9 dorsal hemisection. The PCL/f-MWCNT fibers along with and without EA@lip were placed into the lesion site. We used a PCL/f-MWCNT scaffold with a size of 6 mm × 3 mm. The liposome particles contained 57.5 µg/ml EA and each rat received 250 µl/kg of EA@lip on a 6 × 3 mm scaffold piece. Muscle and skin were closed singly using with Vicryl 3.0 suture. The twenty-four animals were randomly separated into four groups as described follow: (1) the Ctrl-operated group that underwent laminectomy without injury (Ctrl-), (2) the SCI group (Ctrl+), (3) the SCI group that received PCL/f-MWCNT treatment (PCL/CNT), and (4) the SCI rats that received scaffolds containing EA@lip (PCL/CNT/EA).

Post-surgery care

Rats received the antibiotic gentamicin (6 mg/kg, ip) daily for 7 days and buprenorphine hydrochloride (1 mg/kg, subcutaneous) twice a day for 3 days immediately after surgery. They were kept in a room at 27 °C until they regained consciousness. They also received 4 ml of dextrose solution subcutaneously right after surgery and 2.5 ml daily for the next 3 days. Rats were paired throughout survival and their bladders were manually emptied using the Creed maneuver until they started reflex voiding. Rats were cleaned and dried as needed.

Behavioral assessments

OpenField walking

The Basso, Beattie, and Bresnahan (BBB) scale was used to measure the open-field walking ability. The animals were subjected to several sessions in the open field, following which they were scored by two trained observers, who were unaware of the treatment, for a span of 4 min. Scoring were done on the first day after the injury and then every week for 4 weeks. A score of 0 points indicates no hind limb movement, while a score of 21 points reflects normal locomotion.

The contact plantar placement (CPP) test

We applied the CPP method to evaluate how well the SCI rats could integrate sensory and motor information. The test was performed weekly, beginning one week after the injury. We lightly pressed each hind paw's back side to a regular lab bench's edge and measured how often the rat could touch the bench with its foot during three attempts for each hindlimb.

Electrophysiological stimulation and recording

We followed the methods described by Bovet-Carmona et al. to prepare the animals for electrophysiological recordings four weeks after SCI induction [30]. We used pyramidal cells stimulation to induce synaptic inputs from the axons of CA3 neurons in the CA1 region of the hippocampus. We injected the rats with 1.6 g/kg urethane for anesthesia and fixed their heads in stereotaxic frames. We used Paxinos and Watson's atlas to locate CA1 and pyramidal cells pathways on the skull [31], and inserted a bipolar stimulating electrode (stainless steel, 100 µm in diameter, tip separation 500 µm, CFW, USA) in the pyramidal cells. We placed the recording electrode (tungsten, 50 µm in diameter, tip separation 1 mm, CFW, USA) in the CA1 from the skull (coordinates: AP = 3.4 mm, ML = 1.5, DV = 4.45.1, at an angle of 52.5°). We used a two-channel Electromodule amplifier (R12, ScienceBeam) to record the synaptic input of field excitatory postsynaptic potentials (fEPSPs). After a steady baseline recording of synaptic responses for 30 minutes, long term potentiation (LTP) was induced by tetanic stimulation (100 pulses were given at 100 Hz). Synaptic responses were collected 90 minutes later following LTP induction. Response change was measured in % of the slope and amplitude baseline.

Reverse transcription-quantitative polymerase chain reaction (RT-qPCR) analysis

We used a miRNeasy isolation kit (QIAGEN) with on-column DNase treatment (QIAGEN) to isolate total RNA from the hippocampus tissue in this study. The Verso cDNA Kit (Thermo Scientific) was used to generate cDNA from the purified total RNA. We mixed RNA (1 g) with 5 cDNA-synthesis buffer, dNTP mix (0.5 nM final concentration), Verso Enzyme Mix, and random hexamers (400 ng/l), and heated it at 70 °C for 5 min. Then, we incubated the tubes at 42 °C for 30 min and at 95 °C for 2 min. We performed RT-qPCR on an ABI 7900 HT FAST Real Time PCR (Applied Biosystems) using cDNA TaqMan Universal Master Mix II (Applied Biosystems). The reaction conditions included an initial denaturation at 95 °C for 15 min, followed by 40 cycles of denaturation at 95 °C for 10 sec, annealing for 30 sec, and extension for 30 sec. We normalized gene expression to GAPDH and

Table 1. The primer sequences for RT-qPCR

Primer	Sequence (5'-3')	Reference Seq. number
APP	Forward: 5′-TGATCTACGAGCGCATGAAC-3′	NM_019288.2
	Reverse: 5′-AGAAGGCATGAGAGCATCGT -3′	
CNP	Forward: 5′-ATGGGCTCTACAGATACAGACATC-3′	NM_030871.1
	Reverse: 5′-CCTATGGATGTGTGTCAGCATGCT-3′	
GRIK2	Forward: 5′-CCCAGGATGATGTGAACGG-3′	NM_019309
	Reverse: 5′-CCCAGGATGATGTGAACGG-3′	
Munc 18-1	Forward: 5′-AATGCGGCCGCACCCATTGGCCTCAAAGCT-3′	NP_037170.1
	Reverse: 5′-ATTTCTAGATTGTATACATCATTTTCG-3′	
GAPDH	Forward: 5′-TTCACCACCATGGAGAAGGC-3′	NM_017008.4
	Reverse: 5′-GGCATGGACTGTGGTCATGA -3′	

Note: RT-qPCR: reverse transcription-quantitative polymerase chain reaction; APP: amyloid beta precursor protein; CNP: cyclic nucleotide phosphodiesterase; GRIK2: glutamate ionotropic receptor kainate type subunit 2; Munc 18-1: syntaxin-binding protein 1; GAPDH: glyceraldehyde 3-phosphate dehydrogenase

calculated the relative quantity of expression of the target gene based on the comparative Ct method. We repeated these experiments three times. Table 1 summarizes the gene expression assays used in the study.

Statistical

All data were analyzed using Graphpad prism 9.0 statistical software (San Diego, CA, USA). Analysis of variance (tow-way and one–way ANOVA- Tukey's multiple comparisons test) was utilized to evaluate the significance of the obtained results. All experiments were conducted at least three times and data were expressed as the mean ± standard deviation (SD). The statistical significance level was set at $P<0.05$.

RESULTS

Characteristics of EA@lip and PCL/f-MWCNT scaffold

DLS results showed that the size of EA@lip was 129.4 ± 2.05 nm. Also, the TEM image demonstrated that liposomes had almost spherical shape with the homogeneous size of around 100 nm and were almost uniform which were compatible with the results obtained by DLS (Fig. 1a). The FESEM photographs indicated that PCL/f-MWCNT scaffold was composed of randomly oriented, bead-free and uniform nanofibers (Fig. 1b). The mean diameter of PCL/f-MWCNT nanofibers was 243 ± 45 nm. The FESEM image of EA@lip on the surface of PCL/f-MWCNT scaffold indicates all produced nanostructures are almost uniform spherical shapes, with no significant variation in their shapes and sizes (Fig. 1c).

Neurobehavioral function of the animals

To verify whether SCI induction was successful, the BBB and CPP scores in the four groups were examined. All rats behaved normally before modeling. Immediately following the SCI, the injury symptoms were the same for all the rats in

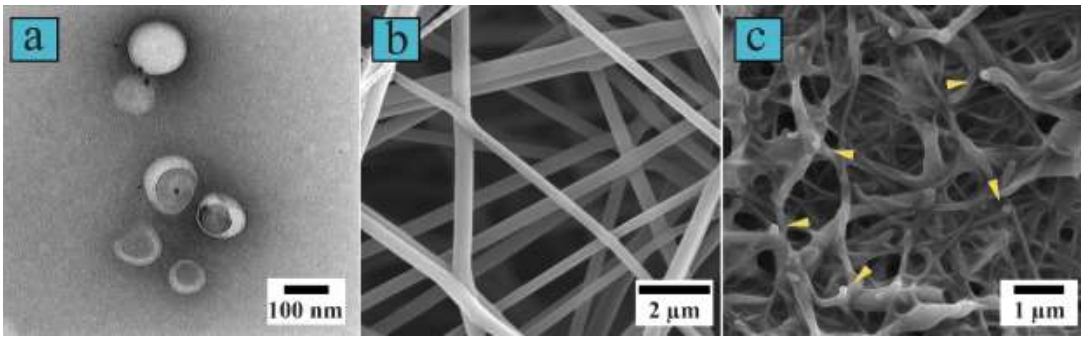

Fig. 1. (a). Transmission electron microscopy images of liposomes. Image demonstrated that liposomes had almost spherical shape with the homogeneous size of around 100 nm. (b). FE-SEM micrographs of PCL/f-MWCNT scaffold. The mean diameter of PCL/f-MWCNT nanofibers was 243 ± 45 nm. (c) FE-SEM image of PCL/f-MWCNT/EA@lip scaffold. Arrowheads indicate liposomes

Table 2. PCL/f-MWCNT scaffold along with EA@lip facilitates the recovery of motor and sensorimotor functions in a rat model of spinal cord injury

Time (days)		Groups			
		Ctrl-	Ctrl+	PCL/CNT	PCL/CNT/EA
1	BBB	20 ± 0.89	0 ± 0	0 ± 0	0 ± 0
	CPP	-	-	-	-
7	BBB	20.5 ± 0.83	1 ± 1.09	2.1 ± 1.3	3 ± 0.89
	CPP	6	0	0.3 ± 0.51	0.6 ± 0.5
14	BBB	20.8 ± 0.4	2.1 ± 1.3	4.3 ± 0.8^{a}	6.3 ± 1.3^{aaaa}
	CPP	6	0.3 ± 0.5	0.83 ± 0.4	1.5 ± 0.54^{aa}
21	BBB	21	4 ± 2.6	6.3 ± 1.5^{a}	8.8 ± 1.8^{aaaa,bb}
	CPP	6	0.6 ± 0.5	1.5 ± 0.83	3.1 ± 0.75^{aaaa,bbb}
28	BBB	21	4.5 ± 2.5	8.1 ± 2.04^{aaaa}	12.1 ± 1.7^{aaaa,bbbb}
	CPP	6	1 ± 0.8	2.3 ± 1.2^{aaa}	3.6 ± 0.51^{aaaa,bbb}

Changes in the Basso, Beattie, and Bresnahan (BBB) and contact plantar placement (CPP) scores over time indicating the improvement of movement and sensation after damage to the spinal cord. Data are presented as mean ± SD (n = 6). a indicate significant differences from the Ctrl+ group and b indicates the difference from PCL/CNT group (^{a}P<0.05, ^{aa}P<0.001, ^{aaa}P<0.001, ^{aaaa}P<0001, ^{b}P<0.05, ^{bb}P<0.01, ^{bbb}P<0.001, and ^{bbbb}P<0.0001). PCL/CNT: treatment with polycaprolactone/ multiwall carbon nanotube functionalized scaffold; PCL/CNT/EA: treatment with PCL/f-MWCNT scaffold covered with liposome containing ellagic acid; Ctrl-: laminectomy without injury; Ctrl+: SCI group without treatment

the Ctrl+, PCL/CNT and PCL/CNT/EA groups, which indicated that the SCI was done correctly. The behavioral scores in all groups are shown in Table 2. Based on BBB scores, the behavioral improvement of the injured groups was similar until the first week. After 2 weeks, a significant improvement was seen in the scaffold receiving groups compared to the Ctrl+ group (P<0.05), however, there was no difference between the two treatment groups. From the third week onwards, the recovery process of the PCL/CNT/EA group overtook the PCL/CNT group (P<0.01).

Also, we monitored the recovery of sensorimotor integration with the CPP test. Our results showed that in the second week, only the PCL/CNT/EA group had a significant movement improvement compared to the Ctrl+ group (P<0.01). In the fourth week, both groups receiving scaffolds had a significant improvement compared to the Ctrl+ group (P<0.001). Also, the PCL/CNT/EA group showed better sensorimotor recovery than the PCL/CNT group from third week onward (P<0.001). In these experiments, rats exhibited gradual recovery of locomotor and sensorimotor functions (Table 2), and PCL/f-MWCNT scaffold along with EA@lip advanced these activities after 4 weeks. The results suggests that implant of PCL/f-MWCNT scaffold along with EA@lip may alleviate SCI and relieve associated symptoms. However, the interventions could not improve the behavior to the level of the Ctrl- group in this period of time.

Scaffold along with liposome alters the LTP in area CA1

Hippocampal LTP has been widely accepted as a candidate cellular mechanism for associative learning and memory. In order to investigate the possible role of PCL/f-MWCNT with/without EA@lip on hippocampus function after SCI, pyramidal cells of the hippocampus were subjected to input recording. Changes in tetanus stimulation fEPSP slope and amplitude in the Ctrl- group indicated that tetanic stimulation was successfully induced. However, in the Ctrl+ group, tetanic stimulation was not induced, as no significant differences were observed in fEPSP amplitude and slope between the pre- and post-tetanus recordings. Changes in slope and amplitude before and after tetanus stimulation show that the groups receiving the scaffold showed improvement in LTP induction compared to the Ctrl+ group (P<0.01). Interestingly, significant changes were seen in the fEPSP slope and amplitude of the PC/CNT/EA group compared to the PC/CNT group (P<0.05) (Fig. 2a and c). However, in the 90 min after tetanus stimulation, only the slope changes between these two groups were significant (P<0.001), not the amplitude. Also, in the 90 min after tetanus stimulation, the treatment in the PCL/CNT/EA group brought fEPSP slope changes closer to the Ctrl- group (P<0.01) and

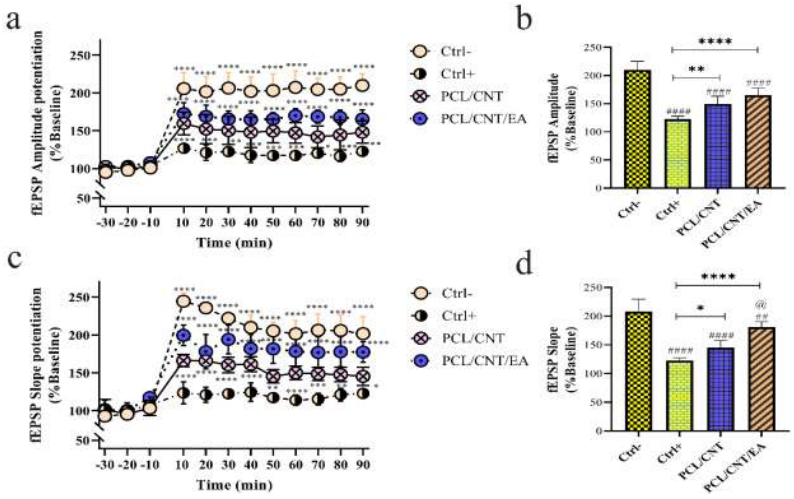

Fig. 2. Long-term potentiation of hippocampus, which is impaired by spinal cord injury (SCI), was restored by PCL/f-MWCNT with EA@lip treatment. (a) Percentage change in field excitatory postsynaptic potential (fEPSP) amplitude. (b) The average percentage change of fEPSP amplitude in 90 min after the tetanus stimulation. (c) Percentage change in fEPSP slope. (d) Average percentage change of fEPSP amplitude in 90 min after the tetanus stimulation. Data are presented as mean ± SD (n = 6). * compared to the Ctrl+ group, # compared to the Ctrl- group and @ compared to the PCL/CNT group ($^{**}P$<0.1, $^{****}P$<0.0001, $^{\#}P$<0.05, $^{\#\#\#}P$<0.001, $^{\#\#\#\#}P$<0.0001, and $^{@}P$<0.001). PCL/CNT: treatment with polycaprolactone/ multiwall carbon nanotube functionalized scaffold; PCL/CNT/EA: treatment with PCL/f-MWCNT scaffold covered with liposome containing ellagic acid; Ctrl-: laminectomy without injury; Ctrl+: SCI group without treatment

increased the fEPSP slope and amplitude compared to the Ctrl+ group (P<0.0001) that indicated treatment with PCL/f-MWCNT scaffold combined with EA@lip can improve LTP in hippocampus after SCI (Fig. 2b and d).

Altered expression profiles of mRNAs in the hippocampus after SCI

Four weeks after the injury, in the Ctrl+ and PCL/CNT groups, mRNA expression of APP (Fig. 3a) and GRIk2 (Fig. 3c) increased, whereas expression

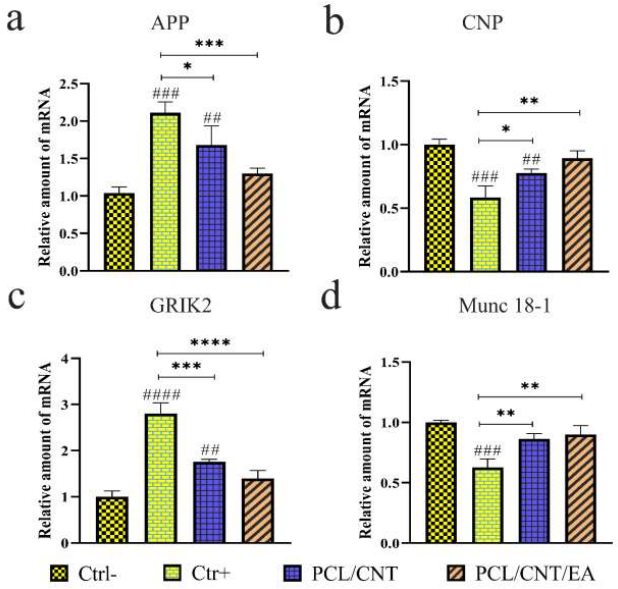

Fig. 3. Quantification expressed mRNA in the hippocampus four week after spinal cord injury (SCI) by RT-qPCR. (a) Relative amount of mRNA of (a) APP, (b) CNP, (c) GRIK2, and (d) Munc 18-1 genes. Data are presented as mean ± SD (n = 3). # Compared to the Ctrl- group and * compared to the Ctrl+ group ($^{\#\#}P$<0.01, $^{\#\#\#}P$<0.001, $^{\#\#\#\#}P$<0.0001, $^{*}P$<0.05, $^{**}P$<0.001, $^{***}P$<0.001, and $^{****}P$<0.0001). PCL/CNT: treatment with polycaprolactone/ multiwall carbon nanotube functionalized scaffold; PCL/CNT/EA: treatment with PCL/f-MWCNT scaffold covered with liposome containing ellagic acid; Ctrl-: laminectomy without injury; Ctrl+: SCI group without treatment; APP: amyloid beta precursor protein; CNP: cyclic nucleotide phosphodiesterase; GRIK2: glutamate ionotropic receptor kainate type subunit 2; Munc 18-1: syntaxin-binding protein 1

of CNP (Fig. 3b) and Munc 18-1 (Fig. 3d) decreased, compared to the Ctrl- group (P<0.001, P<0.0001, P<0.001, and P<0.001, respectively). Nevertheless, the mRNA levels of the mentioned genes in the PCL/CNT/EA group were able to reach the level of the Ctrl- group. These results revealed that PCL/f-MWCNT scaffold implantation with EA@lip improves neurogenesis in the hippocampus after spinal cord injury.

DISCUSSION

One area of interest in SCI research is the occurrence of cognitive deficits and problems with memory functions. These issues have gained more attention in recent years due to changes in the structural of the SCI patients, which has seen the average age at injury and age of patients living with injury increase. Especially, individuals with SCI are at a significantly higher risk of cognitive impairments with a reduced ability to learn new practices and maintains memories, along with a decline in information processing rate, visual memory, and perceptual reasoning [14, 32]. The hypothesis is that the impaired cognition and memory loss seen in SCI patients, compared to healthy people of the same age, may be related to a decrease in the formation of new neurons in the hippocampus. Also according to some studies, changes in synaptogenesis in a region of central nervous system are considered responsible for impairs inputs in hippocampus [5]. In this study, we measured the effects of PCL/f-MWCNT scaffold along with EA@lip on genes expression changes related to hippocampal memory and cognition and hippocampal plasticity impairment induced by SCI. Our results indicate that PCL/f-MWCNT/EA@lip scaffold improves post-injury behavioral performance. Noted, inputs impairment occurs in CA3-CA1 synapses after SCI. Scaffold treatment effectively enhances hippocampal functional potential. Interestingly, in PCL/CNT/EA group, the expression of CNP and Munc 18-1 genes increased, while the expression of APP and GRIK2 genes decreased to levels comparable to that of the undamaged group.

Liposome size is very important for drug delivery due to controlling the pharmacokinetic behavior of the drug in the body, liposome stability and interaction with cells and tissues. Liposome size for drug delivery to the central nervous system is usually between 50 and 200 nm [33]. TEM and DLS results showed that liposome size is in the appropriate range (130 nm) for spinal cord reconstruction and hippocampal function improvement. Abroumand Gholami [2023, Unpublished manuscript] reported that release of ellagic acid encapsulated in liposome from the PCL/f-MWCNT scaffold surface in PBS solution reached about 71% after 7 days [34]. Also, The FE-SEM images of our study show that the fabricated EA@lip is well distributed in the scaffold fibers and has no aggregation. In addition, fibrous morphology is crucial for tissue engineering scaffolds because this morphology resembles the structure of most human tissues. This structure enhances cell adhesion, differentiation and tissue growth, especially in nerve tissue regeneration [17]. The FE-SEM images indicate that the fibrous structure of the scaffold is well formed and beadless. Also, the diameter of the fibers is a significant factor in the adhesion of native tissue cells to the polymer scaffold. The diameter of fiber in the nano scale for the scaffold improves the connection and communication of cells in the injured area [35]. Our results demonstrated that the diameter of the scaffold fibers (247 nm) is within the range of the extracellular matrix of the nerve tissue [15].

The effects of SCI on cognitive function are complex. The spinal cord contains ascending and descending fasciculi that connect to various brain regions, and SCI can lead to progressive neurodegeneration at the site of injury [36], impacting regions such as the sensorimotor cortex, corticospinal tracts, thalamus, and internal capsule [37, 38]. Behavioral tests have been extensively used to evaluate brain related activities after spinal cord and brain injury in animals, both of which can result in motor function deficits [39, 40]. In our SCI rat model, we assessed the gradual improvement of sensory and motor actions, which was advanced by the use of scaffolds. The behavioral data indicated that the PCL/CNT/EA group showed the greatest locomotor recovery, followed by the PCL/CNT group, while the Ctrl-group exhibited the worst locomotor scores. However, the timeframe of our study was not sufficient to determine the improvement in movement caused by the scaffolds in our injury model. A longer study may be required to observe weekly changes.

The electrophysiological activity in our study demonstrated that PCL/f-MWCNT scaffolds controlled the directionality of neurite outgrowth and altered cellular function. Cellular electrophysiological activity is critical for neurons

as it enables the generation of action potentials necessary for intercellular communication. In particular, hippocampal neurons are highly plastic and form intricate networks involved in memory formation, making them highly studied for their inputs activities and events of synaptogenesis [41]. Our study is the first to demonstrate the electrophysiological changes in the hippocampus following spinal cord injury. If substrate microstructure can influence the gene expression related to action potential function, such as ion channels, it is also likely that microstructure can impact a neurons ability to generate action potentials. According to this, the increase in amplitude and slope after tetanus stimulation in the PCL/CNT group can be attributed to four factors: (1) the PCL electrospun fibers increased the material's surface-to-volume ratio, leading to a higher contact area between cells and the substrate, potentially affecting cell function [16]. (2) The use of nanoparticles, such as CNTs, can also impact cellular function, as CNTs have the ability to transport ions through ion channels that influence electrophysiological function [21]. (3) Incorporation of CNTs into biomimetic scaffolds can improve neural network formation by creating electrical shortcuts between cells [20]. (4) Functionalization of CNTs can control the growth pattern and branching of neural processes, increasing complexity [42].

To bridge the gap between severed nerve fibers after dorsal hemisection SCI, a scaffold material is required to fill the lesion cavity and support axonal regeneration. EA containing liposomes alone cannot provide this function. Although some studies have suggested that EA and other natural polyphenols may have neuroprotective effects on SCI, they are not enough to prevent neuronal loss or restore tissue integrity [43–47] the molecular mechanisms that underlie this regeneration are unknown. Here we perform translational profiling specifically of corticospinal tract (CST. Therefore, we hypothesized that EA alone would have minimal impact on SCI recovery and hippocampal preservation. The significant differences in the functional potential changes of the PCL/CNT group were observed compared to the uninjured control group. LTP is a lasting enhancement in synaptic plasticity that has been extensively studied in the hippocampus neural circuits [25] memory and behavior or mental health disorders are considered as the most frequent effects of severe and moderate TBI. It has been reported that ellagic acid (EA. Our data demonstrated that the application of EA@lip on the scaffold increases the slope and amplitude of fEPSP, potentially leading to the maintenance of hippocampal inputs and restoration of neurological behaviors. These findings are consistent with Farbood et al.'s observations regarding the effectiveness of EA in increasing the slope and amplitude of fEPSP in the hippocampus following traumatic brain injury [25]memory and behavior or mental health disorders are considered as the most frequent effects of severe and moderate TBI. It has been reported that ellagic acid (EA). Recent research has revealed that EA may activate a range of cell signaling pathways to slow down or attenuate the development of neurodegenerative disorders [24, 26]. The increase in LTP and the changes in gene expression observed in the hippocampus of the group receiving EA@lip can be attributed to EA's properties, including inhibition of free radicals, chelation of iron, activation of various cell signaling pathways, and reduction in mitochondrial dysfunction [26].

Our study further showed that EA@lip effectively reduces the expression of APP and GRIK2, demonstrating its potent neuroprotective effects. In the study conducted, it was observed that SCI had a considerable effect on the gene's expression related to memory and cognition in the hippocampus; specifically, expression of APP and GRIK2 decreased, while the expression of CNP and Munc 18-1 genes increased. Previous research has indicated that the increase in the expression of amyloid precursor protein (APP) plays a crucial role in beta-amyloid (Aβ) production and the pathogenesis of Alzheimer's disease [48]. In the context of brain injuries caused by various factors, including SCI, the high expression of APP gene can lead to the formation of (Aβ) and consequently, memory impairment in the hippocampus [6]. Moreover, similar to our findings, another study reported that spinal cord injury can increase APP gene expression and result in hippocampal memory deterioration [49]. Our results showed that the group receiving the scaffold containing CNT experienced a decrease in APP expression in the hippocampus. CNT appears to reduce fibrillation Aβ [50]. Considering the increase of LTP and the decrease of APP gene expression in the PCL/CNT group, we assume that the presence of CNT caused the reduction of Aβ through the

modulation of APP expression. Also, RT-qPCR data showed that EA@lip intensified the inhibitory effect on APP expression. Kiasalari et al. reported that EA inhibits Alzheimer's effects in the model of Aβ injection into the hippocampus through the regulation of pathways unrelated to the APP gene [48]. However, the evidence indicates that EA has reduced the formation of Aβ and increased cognitive memory by reducing the expression of genes related to APP [51].

The gene GRIK2 is known to be involved in encoding kainate-type glutamate receptors, which play a critical role in memory and learning processes in various regions of the brain. Previous studies have suggested that increased expression of GRIK2 can lead to improved glutamate receptor function and enhance memory activity and information transfer in memory mechanisms in the brain [8]. However, our research has shown that excessive expression of the GRIK2 gene is associated with a decline in behavioral performance and a decrease in action potential in the hippocampus. This change in GRIK2 behavior is believed to be the result of spinal cord injury, leading to increased secondary responses in the hippocampus. An increase in GRIK2 gene expression can lead to an increase in the number of kainate receptors, making neurons more sensitive to glutamate stimuli than in the normal state. This heightened sensitivity can cause unnecessary signals. These unnecessary signals may hinder memory storage in the hippocampus, also, the heightened neuron sensitivity can cause a decrease in their ability to detect vital and important signals, resulting in less memory stored in the brain [52, 53]. Qian et al. demonstrated that PCL composite scaffold enhanced nerve tissue regeneration and decreased glutamate levels. The reduction of glutamate toxicity improved motor and electrophysiological functions [54]. In this study, recovery might be attributed to the downregulation of GRIK 2 expression due to the decreased glutamate toxicity mediated by PCL/f-MWCNT scaffold. Moreover, scaffolds containing CNT attenuated glutamate toxicity and protected nerve cells from oxidative stress by increasing nerve growth factors such as brain-derived neurotrophic factor, which are involved in memory maintenance and enhancement and nerve damage repair [19]. However, the scaffold utilized in the PCL/CNT group did not lower the expression of GRIK2 to the level of the Ctrl- group. Our findings indicate that incorporating EA@lip onto the scaffold can effectively decrease GRIK2 expression to levels comparable to those observed in the Ctrl-group. GRIK2 encodes the NR2B subunit of the N-methyl-D-aspartate receptor, which is a type of glutamate receptor. Rahimi-Madisehet al reported that EA has anticonvulsant effects by reducing the expression of NR2B [55]. Our data suggest that EA@lip might modulate the GRIK2 pathway to achieve this effect.

The expression of the Munc 18-1 gene in brain neurons plays a crucial role in controlling certain neural network functions such as neurotransmitter secretion, receptor uptake, and signaling transmission. A decrease in the expression of this gene can result in disruptions in nerve signals and a decline in neuronal network activity [56]. Furthermore, it can cause a reduction in the secretion of neurotransmitters, which can negatively impact the brain's ability to store and retrieve information [57]. The decrease in Munc 18-1 gene expression can also lead to an increase in the level of gamma-aminobutyric acid (GABA) in different regions of the brain. This elevation in GABA levels has been linked to decreased activity in hippocampus memory neurons, resulting in decreased memory performance and recall ability [58]. Thus, a decrease in Munc 18-1 gene expression due to SCI may result in decreased neurotransmitter secretion, an increase in GABA levels, and reduced neuronal activity in hippocampal memory. Our results showed that implantation of scaffolds has been found to increase the expression of the Munc 18-1 gene. Research indicates that adding CNTs to PCL structures can enhance the secretion of neurotrophic components, promote tissue repair, and improve the functioning of the nervous system [18]. These findings suggest that combining CNTs with PCL in scaffolds may hold promise for promoting nervous tissue repair and regeneration by increased neurotransmitter secretion, possibly through increasing the expression of Munc 18-1. Our study found that adding EA@lip to the surface of scaffolds promotes synaptogenesis and increases the expression of Munc 18-1. One of the significant roles of EA in promoting neurological health is by stimulating the secretion of neurotransmitters such as dopamine, serotonin, and norepinephrine [47, 59]. These neurotransmitters play a vital role in regulating nervous activities, and the distribution of their concentrations in different situations helps control nerve activities. Therefore, EA@lip

may contribute to nerve recovery by aiding in the secretion of more neurotransmitters, possibly due to the upregulation of the Munc 1-18 gene.

The expression of the CNP gene is crucial for maintaining the level of myelinated neurons, which are responsible for the rapid transmission of nerve signals between neurons. However, if the expression of the CNP gene decreases, the level of myelination may reduce, leading to a decrease in hippocampal memory [13]. This reduction in myelination may result from a decrease in the number or quality of myelin-producing cells, leading to the production of incomplete myelin that can reduce communication between neurons. The decline in CNP expression may also lead to motor function reduction, synaptogenesis decrease, and LTP decline [12]. The PCL/CNT scaffold has been successfully used as a tissue transport system for neuroregeneration and especially the increase of the myelinated surface. The PCL/MWCNT scaffold has shown promising results in experimentally creating neuronal nucleation, increasing the level of myelin, and improving the function of spinal neurons [17]. Therefore, the PCL/f-MWCNT scaffold has regulated the expression of the CNP gene and improved the functional potential in the hippocampus by preserving myelin. Also, EA has been investigated as a stimulatory agent for neurological and SCI models, where it has been found to significantly increase myelin and promote injury repair [60]. In this study, we observed that implanting the scaffold together with EA@lip increases the BBB and CPP scores and improves the functional potential in the hippocampus. Also, ellagic acid led to an increase in CNP expression to the extent of the Ctrl- group, which showed that the recovery of myelin in the hippocampus was well done.

CONCLUSION

In conclusion, our findings suggest that the implantation of PCL/f-MWCNT scaffold along with EA@lip in the injured spinal cord by activating CNP and Munc 18-1 signaling pathways and inhibiting APP and GRIK2 signaling pathways leads to behavioral improvement and increased LTP by increasing the fEPSP slope and amplitude in the hippocampus. Therefore, PCL/f-MWCNT/EA@lip could be a potential substrate for behavioral improvement and secondary damage to the hippocampus after SCI. The exact function of GRIK2 in hippocampal changes after SCI is unclear because of inconsistent findings. In our experiments, examining the relationship between excitatory strength and synaptic transmission showed that overexpression of GRIK2 decreased the efficiency of synaptic transmission in hippocampus after SCI. Therefore, more research is required to understand how GRIK2 works in hippocampus and to find a better way to treat the neural damage caused by SCI.

ACKNOWLEDGMENTS

The authors would like to thank Mashhad University of Medical Sciences for the financial support of this work.

CONFLICT OF INTEREST

The authors declare that they have no Conflict of interest.

REFERENCES

1. Lopez-Dee Nicola AF, Encinas JM, Labombarda F. Spinal cord injury leads to hippocampal glial alterations and neural stem cell inactivation. Cell Mol Neurobiol. 2022;42(1): 197–215.
2. O'Keefe J. Hippocampal neurophysiology in the behaving animal. 2007;475-568.
3. Murray RF, Asghari A, Egorov DD, Rutkowski SB, Siddall PJ, Soden RJ, et al. Impact of spinal cord injury on self-perceived pre-and postmorbid cognitive, emotional and physical functioning. Spinal Cord. 2007;45(6):429–436.
4. Wu J, Stoica BA, Luo T, Sabirzhanov B, Zhao Z, Guanciale K, et al. Isolated spinal cord contusion in rats induces chronic brain neuroinflammation, neurodegeneration, and cognitive impairment: involvement of cell cycle activation. Cell cycle. 2014;13(15):2446–2458.
5. Liu Y, Zhou L-J, Wang J, Li D, Ren W-J, Peng J, et al. TNF-α differentially regulates synaptic plasticity in the hippocampus and spinal cord by microglia-dependent mechanisms after peripheral nerve injury. J Neurosci. 2017;37(4):871–881.
6. Wu J, Zhao Z, Sabirzhanov B, Stoica BA, Kumar A, Luo T, et al. Spinal cord injury causes brain inflammation associated with cognitive and affective changes: role of cell cycle pathways. J Neurosci. 2014;34(33):10989–11006.
7. Abe H, Saito F, Tanaka T, Mizukami S, Hasegawa-Baba Y, Imatanaka N, et al. Developmental cuprizone exposure impairs oligodendrocyte lineages differentially in cortical and white matter tissues and suppresses glutamatergic neurogenesis signals and synaptic plasticity in the hippocampal dentate gyrus of rats. Toxicol Appl Pharmacol. 2016;290:10–20.
8. So SW, Nixon JP, Bernlohr DA, Butterick TA. RNAseq Analysis of FABP4 Knockout Mouse Hippocampal Transcriptome Suggests a Role for WNT/β-Catenin in Preventing Obesity-Induced Cognitive Impairment. Int J Mol Sci. 2023;24(4): 3381.
9. Tang F, Xiao D, Chen L, Gao H, Li X. Role of Munc18-1 in the biological functions and pathogenesis of neurological disorders. Mol Med Rep. 2021;23(3):1.
10. Jia Y, Wang X, Chen Y, Qiu W, Ge W, Ma C. Proteomic and transcriptomic analyses reveal pathological changes in the entorhinal cortex region that correlate well with

dysregulation of ion transport in patients with alzheimer's disease. Mol Neurobiol. 2021;58:4007–4027.
11. Han Y, Chen L, Guo Y, Wang C, Zhang C, Kong L, et al. Class I HDAC inhibitor improves synaptic proteins and repairs cytoskeleton Through regulating synapse-related genes in vitro and in vivo. Front Aging Neurosci. 2021;12:619866.
12. Zhou B, Zhu Z, Ransom BR, Tong X. Oligodendrocyte lineage cells and depression. Mol Psychiatry. 2021;26(1) 103–117.
13. Antontseva E, Bondar N, Reshetnikov V, Merkulova T. The Effects of Chronic Stress on Brain Myelination in Humans and in Various Rodent Models. Neuroscience. 2020;441: 226–238.
14. Sefiani A, Geoffroy CG. The potential role of inflammation in modulating endogenous hippocampal neurogenesis after spinal cord injury. Front Neurosci. 2021;15:682259.
15. Lam D, Enright HA, Cadena J, Peters SKG, Sales AP, Osburn JJ, et al. Tissue-specific extracellular matrix accelerates the formation of neural networks and communities in a neuron-glia co-culture on a multi-electrode array. Sci Rep. 2019;9(1):4159.
16. Bourke JL, Coleman HA, Pham V, Forsythe JS, Parkington HC. Neuronal electrophysiological function and control of neurite outgrowth on electrospun polymer nanofibers are cell type dependent. Tissue Eng Part A. 2014;20(5–6): 1089–1095.
17. Al-Hadeethi Y, Nagarajan A, Hanuman S, Mohammed H, Vetekar AM, Thakur G, et al. Schwann cell-matrix coated PCL-MWCNT multifunctional nanofibrous scaffolds for neural regeneration. RSC Adv. 2023;13(2):1392–1401.
18. Pi W, Zhou L, Zhang W, Liu S, Li C, Zhang M, et al. Three-dimensional conductive polycaprolactone/carbon nanotubes scaffolds for peripheral nerve regeneration. J Mater Sci. 2022;57(24):11289–11299.
19. Huang B. Carbon nanotubes and their polymeric composites: The applications in tissue engineering. Biomanufacturing Rev. 2020;5(1):3.
20. Barrejón M, Rauti R, Ballerini L, Prato M. Chemically cross-linked carbon nanotube films engineered to control neuronal signaling. ACS Nano. 2019;13(8):8879–8889.
21. Rastogi SK, Kalmykov A, Johnson N, Cohen-Karni T. Bioelectronics with nanocarbons. J Mater Chem B. 2018; 6(44):7159–7178.
22. Gupta VK, Kumar R, Nayak A, Saleh TA, Barakat MA. Adsorptive removal of dyes from aqueous solution onto carbon nanotubes: A review. Adv Colloid Interface Sci. 2013;193–194:24–34.
23. Zhijiang C, Cong Z, Jie G, Qing Z, Kongyin Z. Electrospun carboxyl multi-walled carbon nanotubes grafted polyhydroxybutyrate composite nanofibers membrane scaffolds: Preparation, characterization and cytocompatibility. Mater Sci Eng C. 2018;82:29–40.
24. Uzar E, Alp H, Cevik MU, Fırat U, Evliyaoglu O, Tufek A, et al. Ellagic acid attenuates oxidative stress on brain and sciatic nerve and improves histopathology of brain in streptozotocin-induced diabetic rats. Neurol Sci. 2012;33: 567–574.
25. Farbood Y, Sarkaki A, Dianat M, Khodadadi A, Haddad MK, Mashhadizadeh S. Ellagic acid prevents cognitive and hippocampal long-term potentiation deficits and brain inflammation in rat with traumatic brain injury. Life Sci. 2015;124:120–127.
26. Ahmed T, N Setzer W, Fazel Nabavi S, Erdogan Orhan I, Braidy N, Sobarzo-Sanchez E, et al. Insights into effects of ellagic acid on the nervous system: a mini review. Curr Pharm Des. 2016;22(10):1350–1360.
27. Najafi A, Taheri RA, Mehdipour M, Martínez-Pastor F, Rouhollahi AA, Nourani MR. Improvement of post-thawed sperm quality in broiler breeder roosters by ellagic acid-loaded liposomes. Poult Sci. 2019;98(1):440–446.
28. Sou K, Inenaga S, Takeoka S, Tsuchida E. Loading of curcumin into macrophages using lipid-based nanoparticles. Int J Pharm. 2008;352(1):287–293.
29. Babaloo H, Ebrahimi-Barough S, Derakhshan MA, Yazdankhah M, Lotfibakhshaiesh N, Soleimani M, et al. PCL/gelatin nanofibrous scaffolds with human endometrial stem cells/Schwann cells facilitate axon regeneration in spinal cord injury. J Cell Physiol. 2019;234(7):11060–11069.
30. Bovet-Carmona M, Menigoz A, Pinto S, Tambuyzer T, Krautwald K, Voets T, et al. Disentangling the role of TRPM4 in hippocampus-dependent plasticity and learning: an electrophysiological, behavioral and FMRI approach. Brain Struct Funct. 2018;223(8):3557–3576.
31. Paxinos G, Watson CRR, Emson PC. AChE-stained horizontal sections of the rat brain in stereotaxic coordinates. J Neurosci Methods. 1980;3(2):129–149.
32. Chiaravalloti ND, Weber E, Wylie G, Dyson-Hudson T, Wecht JM. Patterns of cognitive deficits in persons with spinal cord injury as compared with both age-matched and older individuals without spinal cord injury. J Spinal Cord Med. 2020;43(1):88–97.
33. Liu P, Chen G, Zhang J. A Review of Liposomes as a Drug Delivery System: Current Status of Approved Products, Regulatory Environments, and Future Perspectives. Molecules. 2022;27(4):1372.
34. Arman Abroumand Gholami. Liposomal ellagic acid transplanted on polycaprolactone/Functionalized multiwall-carbon nanotube scaffold. Unpubl Manuscr. 2023.
35. Tian F, Hosseinkhani H, Hosseinkhani M, Khademhosseini A, Yokoyama Y, Estrada GG, et al. Quantitative analysis of cell adhesion on aligned micro-and nanofibers. J Biomed Mater Res Part A. 2008;84(2):291–299.
36. Li Y, Cao T, Ritzel RM, He J, Faden AI, Wu J. Dementia, depression, and associated brain inflammatory mechanisms after spinal cord injury. Cells. 2020;9(6):1420.
37. Hu X, Wu L, Wen Y, Liu J, Li H, Zhang Y, et al. Hippocampal Mitochondrial Abnormalities Induced the Dendritic Complexity Reduction and Cognitive Decline in a Rat Model of Spinal Cord Injury. Oxid Med Cell Longev. 2022; 4:2022.
38. Hou J, Xiang Z, Yan R, Zhao M, Wu Y, Zhong J, et al. Motor recovery at 6 months after admission is related to structural and functional reorganization of the spine and brain in patients with spinal cord injury. Hum Brain Mapp. 2016;37(6):2195–2209.
39. Peng R-J, Jiang B, Ding X-P, Huang H, Liao Y-W, Peng G, et al. Effect of TNF-α inhibition on bone marrow-derived mesenchymal stem cells in neurological function recovery after spinal cord injury via the Wnt signaling pathway in a rat model. Cell Physiol Biochem. 2017;42(2):743–752.
40. Wang X, Jiao X, Liu Z, Li Y. Crocetin potentiates neurite growth in hippocampal neurons and facilitates functional recovery in rats with spinal cord injury. Neurosci Bull. 2017;33:695–702.
41. Wang H-X, Gerkin RC, Nauen DW, Bi G-Q. Coactivation and timing-dependent integration of synaptic potentiation and depression. Nat Neurosci. 2005;8(2):187–193.
42. Barrejón M, Zummo F, Mikhalchan A, Vilatela JJ, Fontanini M, Scaini D, et al. TEGylated Double-Walled Carbon Nanotubes as Platforms to Engineer Neuronal Networks. ACS Appl Mater Interfaces. 2022;15(1):77–90.
43. Poplawski GHD, Kawaguchi R, Van Niekerk E, Lu P, Mehta N, Canete P, et al. Injured adult neurons regress to an

embryonic transcriptional growth state. Nature. 2020; 581(7806):77–82.
44. Anjum A, Yazid MD, Fauzi Daud M, Idris J, Ng AMH, Selvi Naicker A, et al. Spinal Cord Injury: Pathophysiology, Multimolecular Interactions, and Underlying Recovery Mechanisms. Int J Mol Sci. 2020;21(20):7533.
45. Wertheim L, Edri R, Goldshmit Y, Kagan T, Noor N, Ruban A, et al. Regenerating the Injured Spinal Cord at the Chronic Phase by Engineered iPSCs-Derived 3D Neuronal Networks. Adv Sci. 2022;9(11):2105694.
46. Khodaei F, Khoshnoud MJ, Heidaryfar S, Heidari R, Karimpour Baseri MH, Azarpira N, et al. The effect of ellagic acid on spinal cord and sciatica function in a mice model of multiple sclerosis. J Biochem Mol Toxicol. 2020;34(11): 22564.
47. Ardah MT, Bharathan G, Kitada T, Haque ME. Ellagic acid prevents dopamine neuron degeneration from oxidative stress and neuroinflammation in MPTP model of Parkinson's disease. Biomolecules. 2020;10(11):1–17.
48. Kiasalari Z, Heydarifard R, Khalili M, Afshin-Majd S, Baluchnejadmojarad T, Zahedi E, et al. Ellagic acid ameliorates learning and memory deficits in a rat model of Alzheimer's disease: an exploration of underlying mechanisms. Psychopharmacology (Berl). 2017;234:1841–1852.
49. Faden AI, Wu J, Stoica BA, Loane DJ. Progressive inflammation-mediated neurodegeneration after traumatic brain or spinal cord injury. Br J Pharmacol. 2016; 173(4):681–691.
50. Li H, Luo Y, Derreumaux P, Wei G. Carbon Nanotube Inhibits the Formation of β-Sheet-Rich Oligomers of the Alzheimer's Amyloid-β(16-22) Peptide. Biophys J. 2011; 101(9):2267–2276.
51. Zhong L, Liu H, Zhang W, Liu X, Jiang B, Fei H, et al. Ellagic acid ameliorates learning and memory impairment in APP/PS1 transgenic mice via inhibition of β-amyloid production and tau hyperphosphorylation. Exp Ther Med. 2018;16(6): 4951–4958.
52. Nishizawa Y. Glutamate release and neuronal damage in ischemia. Life Sci. 2001; 69(4): 369–81.
53. Lalo U, Koh W, Lee CJ, Pankratov Y. The tripartite glutamatergic synapse. Neuropharmacology. 2021;199: 108758.
54. Qian Y, Wang X, Song J, Chen W, Chen S, Jin Y, et al. Preclinical assessment on neuronal regeneration in the injury-related microenvironment of graphene-based scaffolds. npj Regen Med. 2021;6(1):31.
55. Rahimi-Madiseh M, Lorigooini Z, Boroujeni SN, Taji M, Amini-Khoei H. The Role of the NMDA Receptor in the Anticonvulsant Effect of Ellagic Acid in Pentylenetetrazole-Induced Seizures in Male Mice. Behav Neurol. 2022; 11: 2022.
56. Margiotta A. Role of SNAREs in neurodegenerative diseases. Cells. 2021; 10(5):991.
57. Santos TC, Wierda K, Broeke JH, Toonen RF, Verhage M. Early golgi abnormalities and neurodegeneration upon loss of presynaptic proteins Munc18-1, Syntaxin-1, or SNAP-25. J Neurosci. 2017;37(17):4525–4539.
58. Vadisiute A, Meijer E, Szabó F, Hoerder-Suabedissen A, Kawashita E, Hayashi S, et al. The role of snare proteins in cortical development. Dev Neurobiol. 2022;82(6):457–475.
59. Huang X, Li W, You B, Tang W, Gan T, Feng C, et al. Serum metabonomic study on the antidepressant-like effects of ellagic acid in a chronic unpredictable mild stress-induced mouse model. J Agric Food Chem. 2020;68(35):9546–9556.
60. Fazlin Z, Myo T, Fauzi DM, Resni M, Noorzaid M. Neuroprotective Effects of Ellagic Acid, Rutin and p-Coumaric Acid on Diabetic Neuropathy Rats. Asian J Med Heal Sci Vol. 2022;5(2):43.